



Inverted VLS Spectrometer at BESSY for Molecular Potential Energy Surfaces and Excitations

Annette Pietzsch, Andrey Sokolov, Thomas Blume, Stefan Nepl, Friedmar Senf, Frank Siewert & Alexander Föhlisch

To cite this article: Annette Pietzsch, Andrey Sokolov, Thomas Blume, Stefan Nepl, Friedmar Senf, Frank Siewert & Alexander Föhlisch (2018) Inverted VLS Spectrometer at BESSY for Molecular Potential Energy Surfaces and Excitations, Synchrotron Radiation News, 31:2, 20-25, DOI: [10.1080/08940886.2018.1435952](https://doi.org/10.1080/08940886.2018.1435952)

To link to this article: <https://doi.org/10.1080/08940886.2018.1435952>



Copyright Taylor & Francis



Published online: 04 Apr 2018.



Submit your article to this journal [↗](#)



Article views: 412



View related articles [↗](#)



View Crossmark data [↗](#)

Inverted VLS Spectrometer at BESSY for Molecular Potential Energy Surfaces and Excitations

ANNETTE PIETZSCH,¹ ANDREY SOKOLOV,² THOMAS BLUME,¹ STEFAN NEPPL,³
FRIEDMAR SENF,³ FRANK SIEWERT,² AND ALEXANDER FÖHLISCH^{1,3}

¹Institute Methods and Instrumentation for Synchrotron Radiation Research, Helmholtz-Zentrum Berlin, Berlin, Germany

²Department Precision Gratings, Helmholtz-Zentrum Berlin, Berlin, Germany

³Institute for Physics and Astronomy, Universität Potsdam, Potsdam, Germany

Introduction

In chemistry, active sites are typically centered at specific functional groups interacting with, e.g., the molecular backbone or the solvent environment. Selectivity and rate are governed by dynamic pathways on the potential energy surfaces of products, educts, and intermediaries. Thus, detailed information on the potential energy surfaces around active atomic centers holds the key to rate and selectivity. Resonant inelastic X-ray scattering (RIXS) allows us to gain this insight, since it accesses, next to electronic and vibronic excitations, spectral losses of purely structural excitations [1]. Through the transient structural distortion in the core excited state, vibrational and rotational RIXS losses are induced and the ground-state potential energy surface is described at selected atomic sites [2–6]. The RIXS spectrum is multidimensional, with not only the energy of the incident and scattered photons as coordinates, but also the polarization state and scattering angle [7]; polarization of the incident radiation gives rise to angular anisotropy of the scattering, which can be exploited to gain information about orbital symmetries in molecules [8]. RIXS is a sub-natural linewidth method with stringent symmetry selection rules, which can even be sharpened upon detuning [9] and can be interpreted in the framework of the apparent “scattering duration time” [10]. With the dedicated Momentum and Energy TRansfer RIXS (METRIXS) instrument for molecular science at BESSY, this approach becomes widely applicable for molecules. For ultrafast reactions, we will approach ultimately the transform limit in energy and time at the upcoming hRIXS at the European XFEL.

Sub-natural linewidth RIXS and relevant energy scales in molecules

Figure 1 shows the principle of sub-natural linewidth RIXS. In the core excited intermediate state, the wave packet propagates and nuclear motion is induced due to the change in potential energy, the dynamic structure factor $S(q, \omega)$ describing the inter-particle correlation and their time evolution in the system. Upon core hole decay, the system relaxes to the electronic ground state, thereby populating a number of ground-state vibrational states. From the energy spacing of the vibrational progression, the ground-state potential energy surface along the nuclear coordinate driven by the core excitation can be extracted.

Sub-natural linewidth RIXS thus quantitatively maps ground-state potential energy surfaces and gains information on their shape far from equilibrium.

RIXS as a coherent Raman process conserves both energy and bandwidth of the scattered radiation. Thus, lifetime broadening of the intermediate state as well as the final state does not contribute to the spectrum for scattering back into the electronic ground state of the molecule, and only the incident energy bandwidth defines the spectral resolution.

Spectroscopy of molecular systems in solution is strongly affected by dipole-dipole interaction due to environmental effects. The change of the solute-solvent interaction in the course of the scattering from the

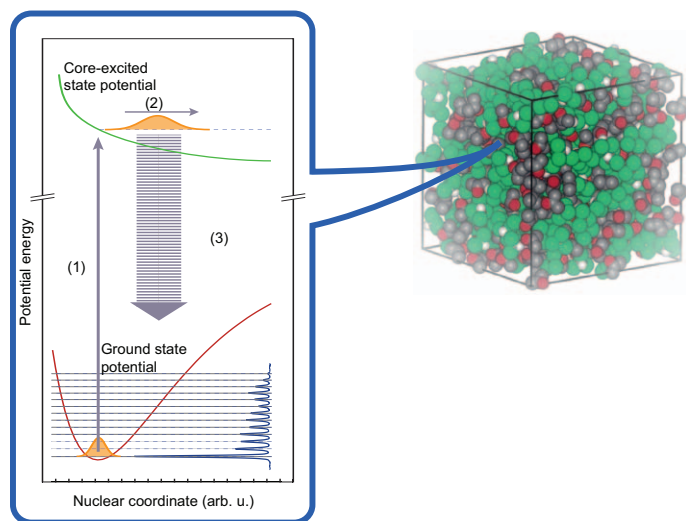
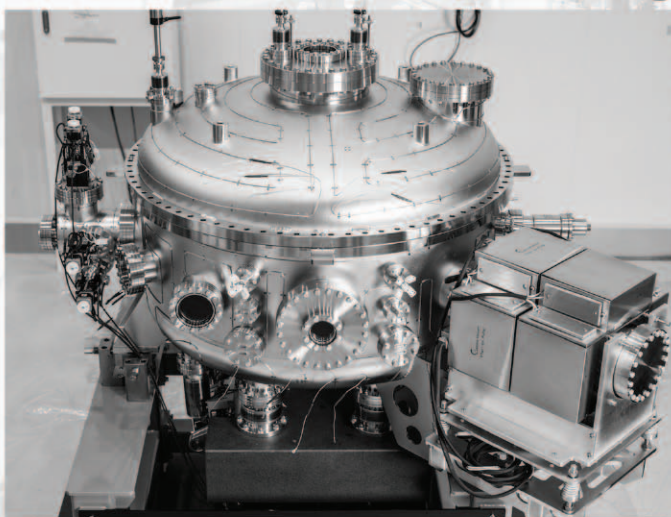


Figure 1: Mapping of potential energy surfaces with sub-natural linewidth RIXS in molecular systems. A molecule is core-excited element specific and site selective in the RIXS process (1). In the intermediate core-excited state, the wave packet propagates and nuclear motion is induced (2). The relaxed wave packet falls back onto the electronic ground state in the core hole decay, thereby populating vibrational states (3). The shape of the ground-state potential energy surface can be extracted from the energy spacing of the vibrational progression along the induced nuclear coordinate. Figure modified from [11].

TOYAMA *Pioneering New Horizons in Science*



Recent Soft X-ray Monochromator project

- Soft and Hard X-ray Monochromators
- Mirror and KB Systems
- Beam Monitors
- Front End Components
- End Stations
- Complete Beamlines
- XFEL Monochromator and Mirror Systems
- XFEL Beam Monitors

If you have a new concept that needs to be developed, then Toyama is the place to come.

Email: sales@toyama-jp.com
Phone: +81-46-579-1411

www.toyama-en.com

ground state via the intermediate state to the final state $0 \rightarrow i \rightarrow f$ modifies the scattering amplitude and leads to an additional broadening $\gamma \rightarrow \gamma + \gamma_s$ [3], defined by the difference of the solvent dipole moments in ground-state μ_0 and final-state μ_f : $\Delta\mu_f = \mu_f - \mu_0$:

$$\gamma_s = \frac{4}{3} \sqrt{\pi \ln 2} |\Delta\mu_f| |\mu_s| \sqrt{\rho/a^3}$$

Here, μ_s is the dipole moment of the solute, ρ is the concentration of the solvent molecules, and a the Weisskopf radius of the solute. If, as in sub-natural linewidth RIXS, the final state is the electronic ground state, the total solvent dipole moment becomes $\Delta\mu_f = \mu_f - \mu_0 = 0$, leading to $\gamma_s = 0$. The environmental broadening is absent and the experimental resolution is only determined by the properties of instrument optics and source, which open for investigation of molecular systems on relevant energy scales.

The average kinetic energy per degree of freedom in a molecule can be estimated by the equipartition theorem, which relates the thermodynamical temperature of a system to its average energies of a fraction of $k_B T$ for each degree of freedom where $k_B = 86 \mu\text{eV/K}$ is the Boltzmann constant. This means that, even for the most advantageous case of a simple gas at room temperature, equipartition leads to $\frac{1}{2} k_B T = 13 \text{ meV}$ per degree of freedom. Molecular aggregates (which are often physiologically relevant) often reach sub-meV scales due to their large

number of coupled degrees of freedom. Chemical reactions, catalytic and biological mechanisms work predominantly on the meV scale at room temperature or 37°C. To excite and follow these processes with a matching energy resolution will give information with thus far inaccessible accuracy on their potential energy surfaces.

Sub-natural linewidth RIXS on molecular water: Directional sensitivity

A single-mode vibrational progression allows mapping the potential energy surface along a specific coordinate. However, when the molecular motion includes several modes, the potential energy surface defined by these degrees of freedom turns into a multidimensional landscape. In these non-deterministic systems, theory breaks down and it becomes non-trivial to obtain information on the shape. Here, experimental methods hold the key to understanding. Selective excitation into different excited states drives certain nuclear motions preferentially [12]. The vibrational progression from sub-natural linewidth RIXS represents a cut through the multidimensional energy landscape along the excited nuclear coordinate.

We illustrate this on the water molecule which we have investigated using sub-natural linewidth RIXS combined with high-level, ab-initio calculations [12, 13].

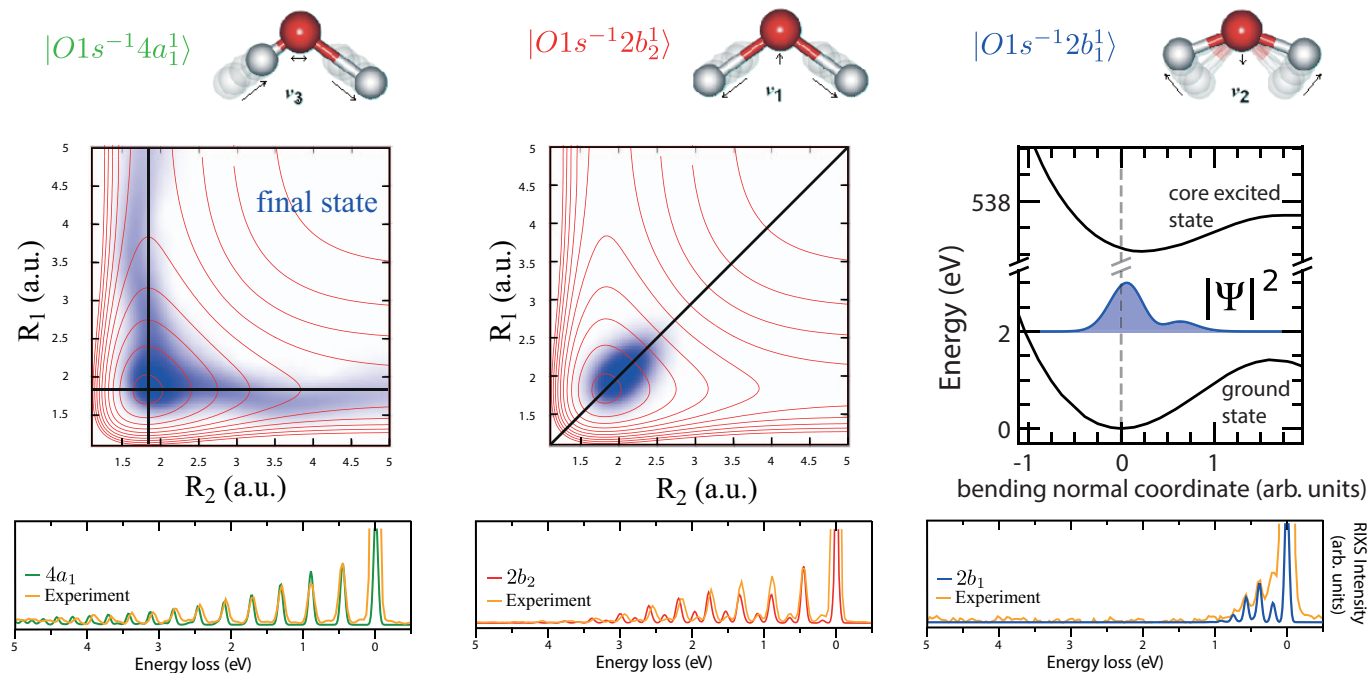


Figure 2: Potential energy surface mapping in multiple dimensions in gas-phase water. The $4a_1$ excited state induces an asymmetric stretch motion along one O-H bond (left), while the $2b_2$ induces a symmetric stretch with a simultaneous elongation of both O-H bonds (middle). Excitation into the $2b_1$ excited state, in turn, induces a pure bending motion (right). Decay of the excited state onto the ground-state potential energy surface results in mapping the ground-state potential energy surface in a cut along the excited coordinate. Calculations are compared to the experimental data in the lower panels. Figure modified from [12, 13].

Water as a 3-atomic molecule has three normal vibrational modes: the symmetric stretch ν_1 , the bend ν_2 , and the asymmetric stretch ν_3 . While the bending frequency is significantly lower, the symmetric and asymmetric stretch frequencies are very close lying, separated only by 12 meV, which cannot be resolved in subnatural linewidth RIXS yet. But selective excitation into different core excited states determines the preferential mode to be driven, as shown in Figure 2.

However, by excitation into different excited intermediate states, we can selectively gate which modes are excited preferentially in the molecule [12]. This is illustrated in Figure 2. Core excitation from the ground-state into the excited-state $4a_1$ drives the asymmetric stretch motion ν_3 . Upon decay, the relaxed wave packet populates the vibrational levels along one elongated O-H bond on the ground-state potential energy surface, representing a cut along this coordinate (left). Excitation into the $2b_2$ excited state drives, in turn, the symmetric stretch vibration ν_1 , elongating both O-H bonds equally. Sub-natural linewidth results in a diagonal cut through the ground-state potential energy surface (middle). Core excitation into the $2b_1$ excited state does not induce a stretch motion, but leads to a change in the bending angle (ν_2), providing a cut through the ground-state potential energy surface along the bending coordinate (right).

This mode-gating effect can be observed in many polyatomic molecules as a general phenomenon, since the directional dependency of spatial distribution differs between ground- and excited-state potential

energy surfaces, resulting in different spatial distribution of the corresponding nuclear wave packets.

The inverted VLS spectrometer

The application of sub-natural linewidth RIXS to molecules to achieve high resolving power is a necessity for maximum resolution of the vibrational progressions. Thus, stability of the instrument is a key factor. To keep the eigenfrequencies of the structure high, we decided against a traditional spectrometer design where the light is reflected upwards, leading to high heavy frames and long arms, and instead mounted the reflective element face down with the light reflected towards the floor.

For a simple and easy-to-align spectrometer with well-known properties, we use a spherical variable linespace (VLS) grating that is mounted face down: the inverted VLS spectrometer.

Source and beamline

The METRIXS spectrometer will be located at beamline U41-SGM of BESSY II, Berlin, which is currently under construction. The beamline provides linearly polarized light from 180 eV to 1600 eV using three spherical gratings with 1200 lines/mm, 1500 lines/mm, and 1800 lines/mm, respectively, and a 10 μm exit slit, resulting in a photon flux of about $3 \cdot 10^{11}$ photons/(s \cdot 0.1% BW \cdot 100 mA). The gratings will be provided by our in-house grating production [14]. Ray tracing shows

that a spot size of $1.5 \mu\text{m} \times 9 \mu\text{m}$ (vertical \times horizontal) can be reached. In a second phase upgrade, a new UE-32 APPLE-II type undulator will be installed.

Spectrometer optical design

The METRIXS spectrometer has a total length of 7.5 m. The spectrometer can be rotated continuously around the beamline focus from 35° to 120° , allowing investigation of the non-dipole terms of molecular transitions in dependence of the scattering angle to gain information on orbital symmetries. In molecular aggregates, even correlation lengths on the nanometer scale can be accessed. A rotational sample chamber similar to that from the VERITAS spectrometer at the MAX IV Laboratory, Sweden, will be used [15].

The optical design scheme is shown in Figure 3. To keep transmission as high as possible with a rather simple and therefore fast alignment process, the METRIXS spectrometer consists of a single optical element: source—spherical VLS grating—detector.

Grating

The spectrometer has two slots for in-situ exchangeable gratings of the size $220 \times 50 \times 50 \text{ mm}^3$. The parameters for the first spherical VLS grating G_1 , which covers the whole energy range from 250 eV to 1000 eV, are given in Table 1. The second slot stays available for future step-forward developments, such as a multilayer coated blazed facet [16] or a VLS grating with extremely high varying parameters.

The parameters of the grating were calculated with the help of the software package GeneVLS/TraceVLS [17] and proofed and adjusted with extensive ray tracing in RAY [18]. Optimization of the VLS coefficients was done on a central energy range to provide best transmission

Table 1: Specified parameters for grating G_1 .

Grating	G_1
Line density N [1/mm]	3000
Laminar profile with groove depth [nm]	5.5
Radius on grating substrate R [mm]	68 982
VLS parameters ($P(x) = N + a_1x + a_2x^2 + a_3x^3$):	
a_1	0.42087
a_2	4.23E-05
a_3	9.488E-08

and with retractions for minimal $r_1 > 900 \text{ mm}$, optical resolving power better than 30000 in the whole range, detector inclination angle in the range $10\text{--}20$ degrees, and a total instrument length of 7.5 m.

Detector

The photons are detected in grazing incidence with a multichannel plate (MCP) coupled to a delay line detector. Three MCPs of $80 \times 50 \text{ mm}^2$ are connected to reach a total detector area of $240 \times 50 \text{ mm}^2$. This increases the horizontal detection angle significantly compared to a standard in-vacuum CCD, which usually has a detection area of one square inch ($2.54 \times 2.54 \text{ mm}^2$). The detector is marked as a green rectangle in the upper panel of Figure 3 with its minimum and maximum positions. The effective pixel size of MCP is assumed to be $\sim 10 \mu\text{m}$. In order to improve resolving power, the detector is inclined relative to the incident beam to a grazing angle in the range of $10^\circ\text{--}20^\circ$. Thus, e.g., for 1000 eV, each pixel covers 9.6 meV, which means that the detector is able to support a spectrometer resolution of 30,000.

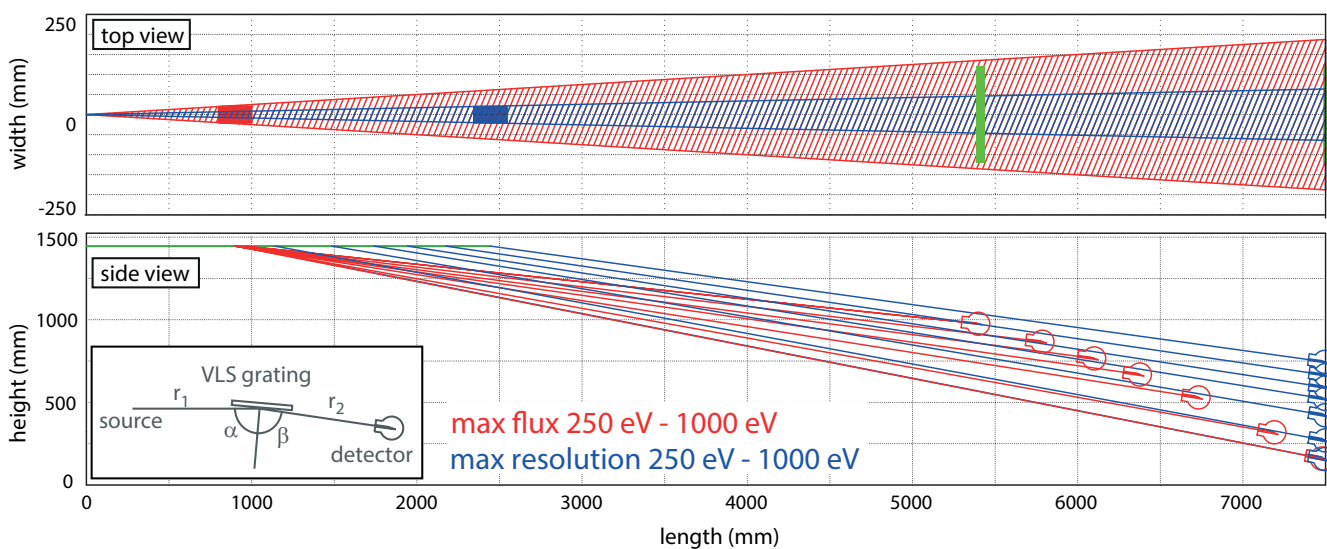


Figure 3: Optical design concept of the inverted VLS spectrometer (inset). The photon beam path is shown from the top and side. The VLS grating is mounted face down for increased mechanical stability; the minimum and maximum grating positions are shown as red and blue rectangles in the upper panel. The green rectangles in the top view panel indicate the detector size relative to the size of the photon beam in the spectrometer, as well as the two extreme detector positions.

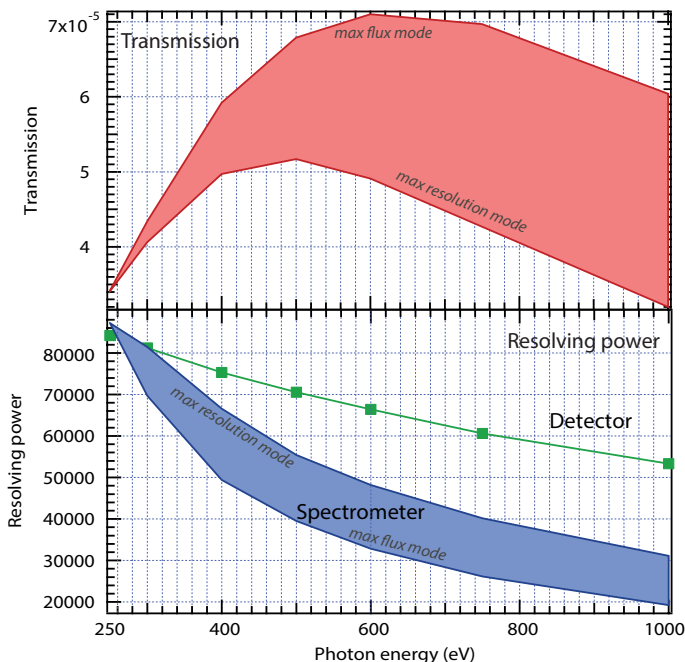


Figure 4: Ray tracing of the resolving power of the METRIXS spectrometer. The two operation modes span an area which is limited at the low-resolution side by the max flux mode and at the high-resolution side by the maximum resolution mode. The ray tracing shows that energy resolution is excellent over the whole detector area.

Stability

The spectrometer design requires a very accurate positioning of the grating and detector to achieve the nominal energy resolution. For this reason, the spectrometer is constructed with a face-down grating to keep as much of the weight from the spectrometer arm close to the beam to reach all grating positions.

The spectrometer will rotate around the sample on spherical bearings, and its position is defined by three fix points: a bearing below the source point, and the two feet that hold the far end of the arm. This is a design that is similar to that of the VERITAS instrument at the MAX IV laboratory. This design has the advantage that, once the grating is positioned on the arm, the whole spectrometer can be rotated without losing sight of the beamline focus and without misaligning the spectrometer.

Operation modes

The METRIXS spectrometer offers two operation modes: focused on maximum flux or maximum resolution. Both modes are available for the whole energy range of the spectrometer, from 250 eV to 1000 eV, and intermediate modes can be accessed if needed. This will allow for tuning the spectrometer to the experimental needs and improving the measurement capability of dilute samples.

The maximum flux mode prioritizes the spectrometer transmission while compromising on the resolving power. The grating is always as close as possible to the sample (r_1 minimal) to increase the solid angle.

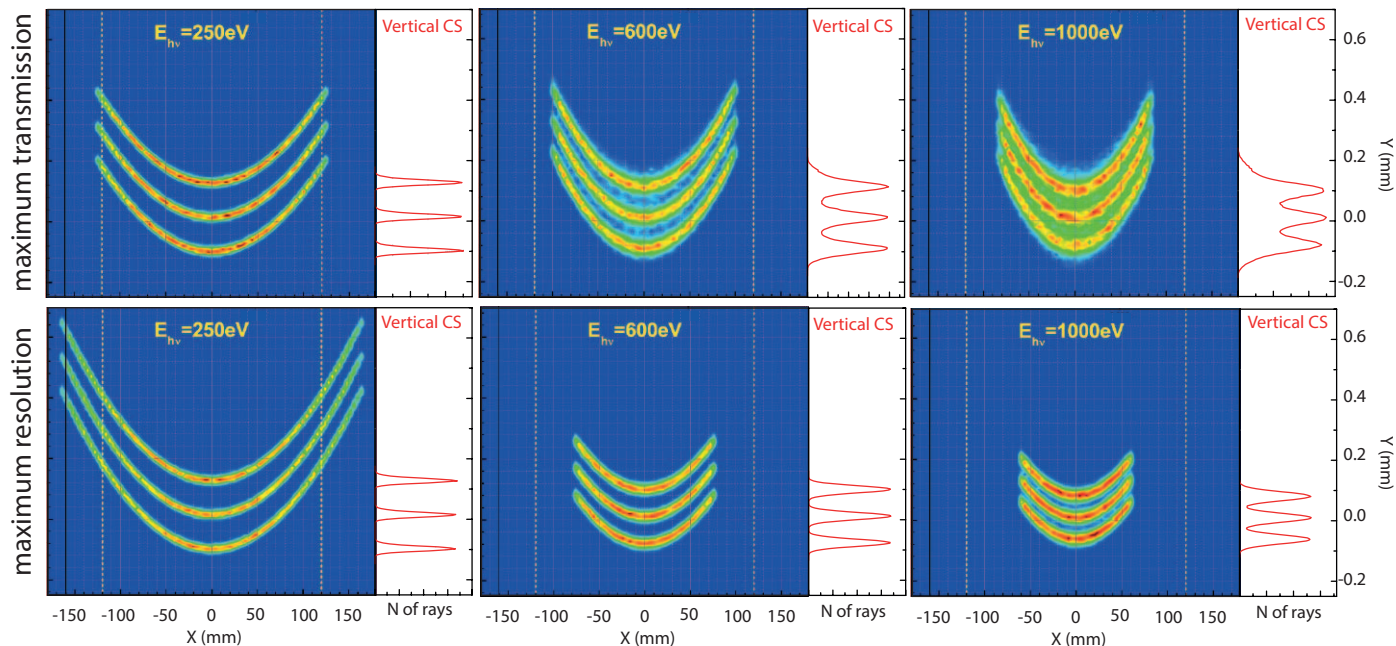


Figure 5: Detector image for different energies and operation modes from ray tracing where the lines have an energy spacing corresponding to a resolving power of 15000 at the respective energy (one-half of the design value). The white dashed lines indicate the detector size. The cross-sections in the side panels represent a cut through the detector at $X = 0$ mm.

Different photon energies are reached by moving the detector along the beam. The maximum resolution mode, in turn, focuses on energy resolution at the cost of spectrometer transmission. Here, the total spectrometer length is kept constant. The spectrometer transmission and resolving power over the whole energy range are presented in Figure 4. The limits of the maximum flux and maximum resolution operation modes are indicated where the red and blue areas define the operation parameter space.

Figure 5 shows the detector images from ray tracing of three selected energies each for the maximum flux and maximum resolution operation modes. The detector width is indicated in dashed lines, showing that its large surface covers the whole spectral image for almost all energies. The three lines have an energy spacing corresponding to a resolving power of 15000 (one-half of the design value) to visualize the spectrometer resolution for the different operation modes. The vertical cross-section in the side panels represents a cut through the line centers at $X = 0$ mm.

Molecule sample environment

The experimental chamber will offer a liquid jet system for radiation-damage-free investigation of molecular samples in solution. The laminar flow region is in the order of a few millimeters before the jet breaks and forms droplets. Either mode can be used for sample delivery. Typical flow rates are 1–2 ml/min, but the use of a gas sheath jet could reduce the flow rate even further. The liquid jet can optionally be equipped with a catcher unit to recycle the sample. Alternatively, a heatable liquid and gas flow cell can be used that we have developed for sub-natural linewidth RIXS applications.

A set of differential pumping stages with pinholes will separate the sample chamber from the beamline vacuum and will allow for maintaining a pressure of $1 \cdot 10^{-3}$ mbar at the sample while keeping $1 \cdot 10^{-9}$ mbar at the refocusing mirrors. The spectrometer grating will be separated from the sample chamber by an ultrathin Si_3N_4 or parylene membrane window, depending on the excitation energy being studied. The membrane is located as close as possible to the sample chamber and its size is tailored to the photon beam diameter to ensure maximum beam transmission.

With the METRIXS spectrometer, we have developed a dedicated spectrometer for sub-natural linewidth RIXS on molecular systems that will optimize the experimental conditions for molecules. This will open a way to map potential energy surfaces of many complex molecular compounds under realistic conditions.

Outlook

With the new inverted VLS spectrometer METRIXS, we will be able to widen the applicability of sub-natural linewidth RIXS on molecules and provide access to ground-state potential energy surface mapping for a wider community. Due to the fact that sub-natural linewidth RIXS is not affected by environmental broadening, the resolving power is solely set by the properties of the spectrometer and beamline optics, as well as the source parameters of the insertion device. With the upcoming new developments on the optics side, such as reflection

zoneplates or multilayer gratings, transmission can be increased up to an order of magnitude without spoiling the energy resolution. Furthermore, in-vacuum undulators will provide higher brilliance and increase the yield in these photon-hungry experiments.

The METRIXS spectrometer will complement the Heisenberg RIXS (hRIXS) spectrometer at the European XFEL in Hamburg, where the additional dimension of time is added to the experiment. There, we will approach and explore sub-natural linewidth RIXS at the transform limit in energy and time.

Acknowledgments

We gratefully acknowledge funding from the Helmholtz Association through the Helmholtz Energy Materials Foundry HEMF and from the ERC-ADG-2014 Advanced Investigator Grant No. 669531 EDAX under the Horizon 2020 EU Framework Programme for Research and Innovation. We thank M. Brzhezinskaya for ray tracing of the beamline and J. Bahrtdt for designing the undulator. The measurements on molecular water were performed together with T. Schmitt at the SAXES instrument of the Swiss Light Source of the Paul Scherrer Institute in Villigen, Switzerland. Our experimental efforts are in close collaboration with the theory groups of F. Gel'mukhanov (KTH, Stockholm) and M. Odelius (Stockholm University). ■

References

1. F. Hennies et al., *Phys. Rev. Lett.* **95**, 163002 (2005).
2. F. Hennies et al., *Phys. Rev. Lett.* **104**, 193002 (2010).
3. Y.-P. Sun et al., *Phys. Rev. B* **84**, 132202 (2011).
4. Y. Harada et al., *Phys. Rev. Lett.* **111**, 193001 (2013).
5. R. C. Couto et al., *Phys. Rev. A* **93**, 032510 (2016).
6. S. Schreck et al., *Sci. Rep.* **6**, 20054 (2016).
7. J.-E. Rubensson et al., *J. Electron Spect. Rel. Phen.* **185**, 294 (2012).
8. S. H. Southworth et al., *Phys. Rev. Lett.* **67**, 1098 (1991).
9. P. Skyyt et al., *Phys. Rev. Lett.* **77**, 5035 (1996).
10. F. Gel'mukhanov and H. Ågren, *Physics Reports* **312**, 87 (1999).
11. A. Pietzsch and A. Föhlisch, *Synchr. Rad. News* **30**, 8 (2017).
12. R. C. Couto et al., *Nat. Comm.* **8**, 14165 (2017).
13. V. V. Cruz et al., *Phys. Chem. Chem. Phys.* **19**, 19573 (2017).
14. F. Siewert et al., *J. Synchrotron Rad.* **25**, 91 (2018).
15. C.-J. Englund et al., *Rev. Sci. Instr.* **86**, 095110 (2015).
16. F. Senf et al., *Optics Express* **24**, 13220 (2016).
17. V. N. Strocov et al., *J. Synchrotron Rad.* **18**, 134 (2011).
18. F. Schäfers, *Springer Series in Modern Optical Sciences* **137**, 9 (2008).

Note

Published with license by Taylor & Francis Group, LLC
© Annette Pietzsch, Andrey Sokolov, Thomas Blume, Stefan Nepl, Friedmar Senf, Frank Siewert, Alexander Foehlich

This is an Open Access article distributed under the terms of the Creative Commons Attribution-Non-Commercial License (<http://creativecommons.org/licenses/by-nc/3.0/>), which permits unrestricted non-commercial use, distribution, and reproduction in any medium, provided the original work is properly cited. The moral rights of the named authors have been asserted.